

Reduced thermal decomposition of OH-free LiNbO₃ substrates even in a dry gas atmosphere

Hirotohi Nagata, Toshihiro Sakamoto, Hideki Honda, and Junichiro Ichikawa
Optoelectronics Division, Sumitomo Osaka Cement Co., Ltd., 585 Toyotomi-cho, Funabashi-shi, Chiba 274, Japan

Eungi Min Haga and Kaori Shima
Central Research Laboratories, Sumitomo Osaka Cement Co., Ltd., 585 Toyotomi-cho, Funabashi-shi, Chiba 274, Japan

Nobuhiko Haga
Faculty of Science, Himeji Institute of Technology, Kamigori-cho, Ako-gun, Hyogo 678-12, Japan

(Received 17 October 1995; accepted 8 March 1996)

A thermal diffusion process of Ti into a LiNbO₃ substrate for optical waveguides has generally been carried out under a wet gas atmosphere in order to prevent undesirable Li outdiffusion. In this work, such thermal decomposition was confirmed to be significantly suppressed for an OH-free LiNbO₃ substrate, even after a dry atmosphere annealing. No extra x-ray diffraction peak for LiNb₃O₈ was detected from the OH-free substrate after 10 h of annealing at 1000°C in a dry O₂. Furthermore, the surface morphology of this sample, and as well an unannealed one, were smooth. In a conventional LiNbO₃ substrate containing many OH ions, subjected to a similar dry annealing, the presence of the LiNb₃O₈ phase and a surface coarsening were observed.

I. INTRODUCTION

Optical waveguide devices based on LiNbO₃ material have become widely used in areas such as optical communication systems and optical measurement applications.^{1,2} Like the proton exchange method at lower temperatures, thermal diffusion of Ti at high temperatures near the Curie temperature of LiNbO₃ is also a common method for forming the optical waveguide on the LiNbO₃ substrate.³⁻⁵ Recently, rare earth ions of Er, Nd, and Yb were codoped with Ti in order to integrate active waveguide devices, such as lasers.^{3,6-13} These high-temperature diffusion processes have been carried out under wet gas atmospheres, O₂ (and N₂), supplied via a water bubbler, in order to suppress a thermal outdiffusion of Li from the substrate surface.¹⁴⁻¹⁶ For the dry or vacuum annealed substrate, the presence of a LiNb₃O₈ phase was reported, which was found to grow heteroepitaxially on the substrate due to decomposition.¹⁶⁻¹⁸ Such a chemically deteriorated layer is considered to be one of the origins for a higher optical propagation loss and dc drift.^{14,19,20}

Compared to the above-mentioned conventional wet annealing process of the LiNbO₃, this paper describes the possibility of a dry annealing process for preparing Ti-diffused waveguides in the OH-free LiNbO₃ substrates without significant surface decomposition. The OH ions were known to be inevitably introduced into the substrate during the growth

and polarization processes of the LiNbO₃ crystal.²¹ The OH-free LiNbO₃ substrates are originally proposed by Koide *et al.* to reduce the Li outdiffusion during the dry annealing.²² They concluded there was reduced thermal degradation in the OH-free substrate, judging from the absence of anomalies in the optical refractive index after the annealing. Here, the absence of the thermally deteriorated layer was confirmed crystallographically. These results strongly indicate that the waveguide formation process, by Ti thermal diffusion, can be performed under a dry gas atmosphere for the OH-free LiNbO₃ substrates. Such a dry annealing process is beneficial not only for the realization of low dc drift devices, as previously reported by the authors, but also to obtain a higher process repeatability.^{5,23,24}

II. EXPERIMENTAL

The OH-free LiNbO₃ substrates used were commercial *z*-cut ones with 3 in. diameters and 0.5 mm thicknesses. A procedure to eliminate OH impurity in the substrate was detailed in Ref. 22. One of the as-received substrates was cut into 15×15 mm² plates for the experiments, hereafter called *ND* samples. Another substrate was annealed at 980°C for 20 h in a wet O₂/N₂ atmosphere to regain OH ions before cutting, called the *NW* samples. A conventional *z*-cut substrate without any OH-free treatment, supplied from a different

TABLE I. Chemical compositions of two different LiNbO₃ substrates supplied from different manufacturers. The sample *N* is an OH-free one mentioned in this paper, while the *Y* is a conventional one containing larger amount of OH ions. The unit in the table is wt. % or ppm

Sample	Li (%)	Nb (%)	Zn (ppm)	Fe (ppm)	Ti (ppm)	Mn (ppm)	Cu (ppm)
<i>N</i>	4.69	62.37	643.0	13.63	2.516	5.682	628.0
<i>Y</i>	4.66	62.61	643.8	10.08	2.671	8.320	633.6

Sample	Ni (ppm)	Cr (ppm)	Co (ppm)	Gd (ppm)	Dy (ppm)	Yb (ppm)	Nd (ppm)
<i>N</i>	41.98	37.43	10.28	10.17	1.034	0.2139	13.59
<i>Y</i>	49.06	32.74	9.942	8.436	1.408	0.1390	17.93

manufacturer, was also prepared for comparison, the *YW* samples. Table I shows chemical compositions of two substrates supplied from the different manufacturers, *N* (i.e., *ND*) and *Y* (i.e., *YW*), in which the amount of Li was measured by atomic absorption spectroscopy (AAS) and the other elements by inductively coupled plasma spectroscopy (ICP). The Li₂O mol % was calculated from Table I as 50.2 mol % for substrate *N* and as 49.9 mol % for *Y*; i.e., both crystals had a stoichiometry composition approximately.²⁵ The OH amounts of the substrates were measured by Fourier transform infrared spectroscopy (FTIR) with peaks around 3480 cm⁻¹.²⁶ The averaged OH absorption coefficient, α was 0.0664 cm⁻¹ for *N* and 1.4627 cm⁻¹ for *Y*, corresponding to a concentration, n , of about 0.2×10^{19} and 4×10^{19} cm⁻³, respectively.²⁷ The content of OH ions was less, by more than ten times, in *N* than in *Y*, showing the substrate *N* had been successfully dehydrated.

The samples *ND*, *NW*, and *YW* were annealed at 600, 800, and 1000 °C, respectively, for 10 h in a dry atmosphere. Three kinds of samples were placed together in a platinum box and loosely covered by a similar box in order to prevent a possible chemical reaction between LiNbO₃ and the SiO₂ materials of the furnace. Throughout the annealing process, O₂ with a dew point less than $\sim 70^\circ\text{C}$ was introduced into the furnace (gas flow rate = 500 cm³/min). Actual dew point of the flowing gas measured at the gas outlet of the furnace was ~ 40 to $\sim 50^\circ\text{C}$ during the heating.

After the annealing, the contents of OH, Li, and Nb in the samples were measured by FTIR, AAS, and ICP methods. For some samples, a secondary ion mass spectroscopy (SIMS) was performed to investigate the depth distribution of Li and Nb near the surface using a Cs⁺ incident ion beam at 5.0 kV and 200 nA. The analyzed area was $90 \times 144 \mu\text{m}^2$. The negative secondary ions of ¹H, ⁶Li, ⁷Li, ¹⁸O, and ⁹³Nb

were detected. X-ray diffraction (XRD) patterns of the samples were observed using Cu K α lines by a conventional $\theta/2\theta$ scan and a rocking curve of the (00,12) peak. The surface morphology was observed by an atomic force microscope (AFM) at ambient atmosphere.

III. RESULTS AND DISCUSSION

A. Chemical analyses of dry annealed samples

In order to confirm the dehydration of the LiNbO₃ samples due to the dry atmosphere annealing, an in situ ¹⁸H₂O mass spectroscopy of the sample while it was heated to 1000 °C at a rate of 10 K/min was carried out in a dry air flowing (50 cm³/min). Figures 1(a) and 1(b) show the results for the samples *N* and *Y*, respectively. Although the sensitivity of the measurement was not very high, the dehydration of the substrate was clearly confirmed beyond 800 °C during the dry heating. The amount of detected ¹⁸H₂O ions was consistently larger for the sample *Y* [Fig. 1(b)] which initially included greater amounts of OH. A direct detection of Li-compound species evaporating from the substrate was also attempted at the same time. However, no corresponding mass peak could be observed for either sample. Because an evaporation of Li₂O over 900 °C was reported as one possible reason for the growth of LiNb₃O₈ at such high temperatures,²⁵ the absence of Li-compound mass peaks in the measurement might be due to mechanical problems such as absorption of the species and absence of negatively charged species. Therefore, *ex situ* chemical and crystallographic analyses were performed for the dry annealed samples to know whether Li-deficient phases were formed or not, as described below.

Table II shows the OH absorption coefficients by FTIR and Li₂O mol % measured for the unannealed and dry annealed *ND*, *NW*, and *YW* samples. Because of the previous

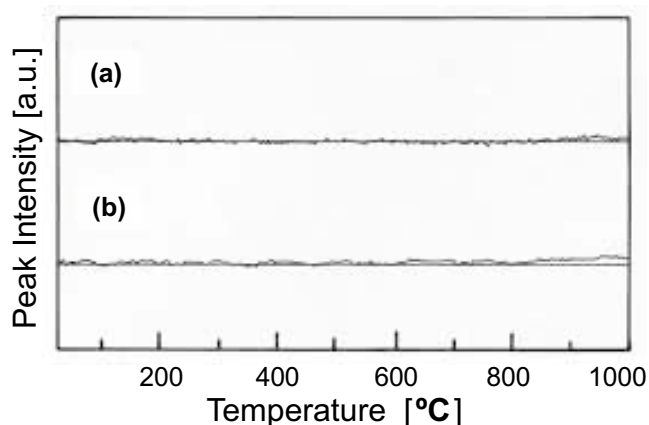


FIG. 1. The relationship between ¹⁸H₂O mass-peak intensity and temperature for the sample *N* (*ND*) in (a) and the *Y* (*YW*) in (b). The LiNbO₃ samples were heated under dry air at a heating rate of 10 K/min.

TABLE II. OH absorption coefficients measured by FTIR and Li₂O molar contents measured by ICP and ASS for unannealed and annealed LiNbO₃ samples.

Sample name	Anneal temp. (°C)	OH absorption coefficient (cm ⁻¹)	Contents of Li and Nb		
			Li (wt. %)	Nb (wt. %)	Li ₂ O (mol %)
<i>ND</i>	Unannealed	0.079	4.69	62.37	50.2
	600	0.086	4.66	62.67	49.9
	800	0.090	4.70	62.94	50.0
	1000	0.088	4.68	62.43	50.1
<i>NW</i>	Unannealed	2.42	4.65	62.46	49.9
	600	0.053	4.65	62.51	49.9
	800	0.070	4.70	62.88	50.0
	1000	0.085	4.70	62.55	50.2
<i>YW</i>	Unannealed	1.77	4.66	62.61	49.9
	600	0.054	4.66	62.73	49.9
	800	0.077	4.69	62.90	50.0
	1000	0.090	4.70	62.66	50.1

wet atmosphere annealing for the OH-free *N* sample (see Sec. II), the initial OH content of the *NW* sample increased to almost the same level as the *YW*. After the 10 h dry annealing at 600, 800, and 1000°C, however, OH contents of the *NW* and *YW* samples decreased significantly and became similar to the *ND* samples, the OH-free ones. The Li₂O contents in the samples were approximately within a stoichiometric regime, and there was no change due to the dry annealing. As a result, although dehydration occurred throughout the samples, it did not cause a significant change in the cationic composition.

In order to check the influence of the annealing on the surface composition, the SIMS measurement was done for the *ND* and *YW* samples, both the unannealed and annealed at 1000°C. The *ND* and *YW* samples correspond to the recently proposed OH-free and the conventional OH-uncontrolled substrates, respectively. The dry annealing temperature of 1000°C was demanded in the waveguide formation process.³ Figures 2 and 3 reveal the SIMS depth profiles for the samples *ND* and *YW*, respectively, on the Li/Nb peak intensity ratio (a) and O/Nb ratio (b). The solid and broken lines denote the results for the unannealed and 1000°C annealed samples, respectively. The depth distribution of the O/Nb ratio was almost identical in all the samples. The Li/Nb ratio for the unannealed samples was greater at the surface of the *ND* substrate. This might be due to the fact that the *ND* substrates had been dry annealed before the polishing process in order to eliminate OH ions,²² and the polishing thickness might not be enough to completely remove the Li-rich layer. In this experiment, the Li/Nb ratio was also increased at the surface due to the dry annealing at 1000°C. The magnitude of the increased Li/Nb ratio was almost the same for both samples. The SIMS results indicated that the surface concentration of

the Li, due to the dry annealing, was greater than expected. However, the depth of the higher Li/Nb region was less than 10 nm as an averaged value for the analyzed area. The Li/Nb ratio through a 1 μm depth was not affected significantly by the dry annealing, as indicated in the results of Table II.

B. XRD analyses of dry annealed samples

The above chemical analyses did not provide proof for the thermal decomposition of the dry annealed samples. Therefore, XRD measurements were carried out to directly investigate a phase decomposition due to the dry annealing at 1000°C. Figure 4 shows the results of the $\theta/2\theta$ scan for the sample *ND* in (a) and *YW* in (b) before (solid line) and after (broken line) the annealing. As seen, only in the annealed *YW* sample, weak peaks ascribed to LiNb₃O₈ phase were detected, suggesting the occurrence of a phase decomposition due to the dry annealing. Judging from the weakness of the detected XRD peaks and the absence of Li reduction in the SIMS result, the extent of the LiNb₃O₈ phase seemed to be very small in area and thin in depth. The XRD rocking curves at the (00,12) diffraction peak were measured for the same samples of Fig. 4. The observed full width of half maximum (FWHM) of the curves were 6 s for all the samples, suggesting no distortion along the z-axis of the remaining LiNbO₃ crystallite after the dry annealing at 1000°C.

Figures 5(a)-5(c) show the other XRD rocking curves for the (00,12) peaks of the samples *ND*, *NW*, and *YW*, respectively. The solid lines denote the results for the unannealed samples, and the broken lines for the corresponding samples annealed at 800°C for 10 h. Concerning the influence of the OH in the LiNbO₃ crystallite, two distinct phenomena could

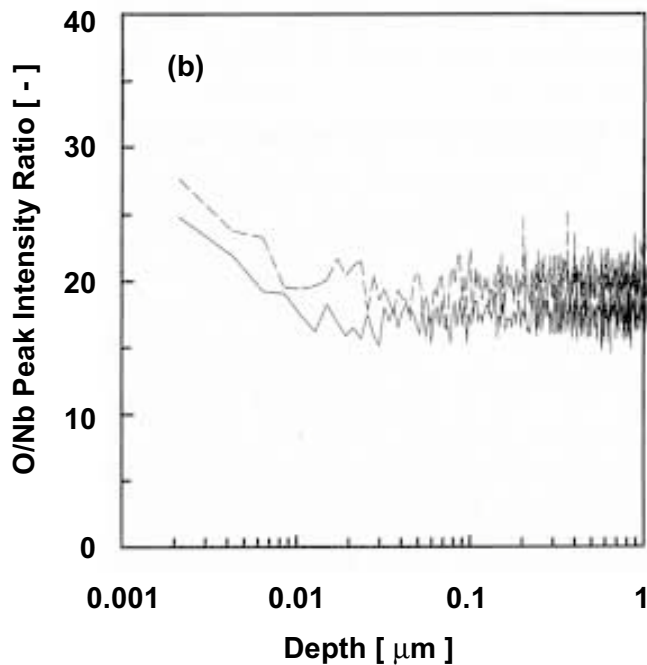
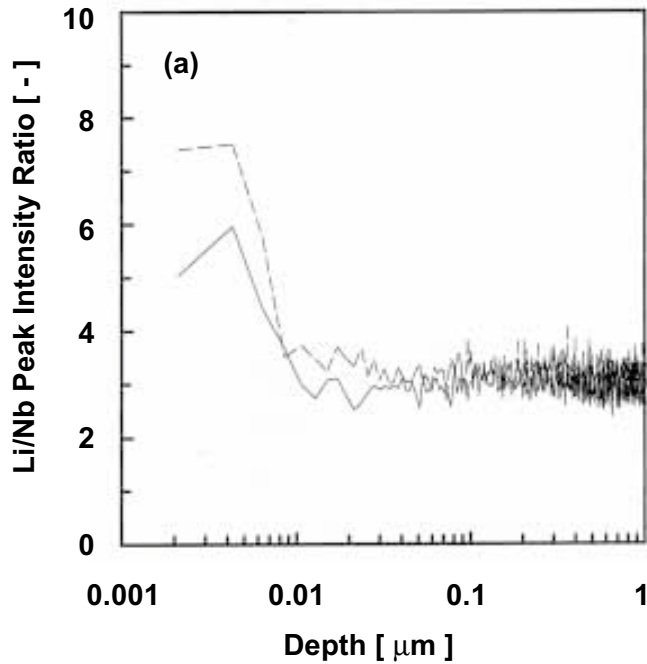


FIG. 2. SIMS peak intensity ratios for (a) Li/Nb and (b) O/Nb. The solid lines denote the unannealed *ND* sample, while the broken lines denote the *ND* sample dry annealed at 1000°C.

be observed from Fig. 5. The first phenomenon was, as shown in the solid curves of Figs. 5(a), *ND*, and 5(b), *NW*, a very slight broadening of the rocking curve toward a lower θ angle (i.e., lattice extension along a z -axis) due to the OH injection into the OH-free substrate by the previous wet annealing. The second one was a large broadening toward a higher θ angle (i.e., lattice shortening along a z -axis) after the dry annealing

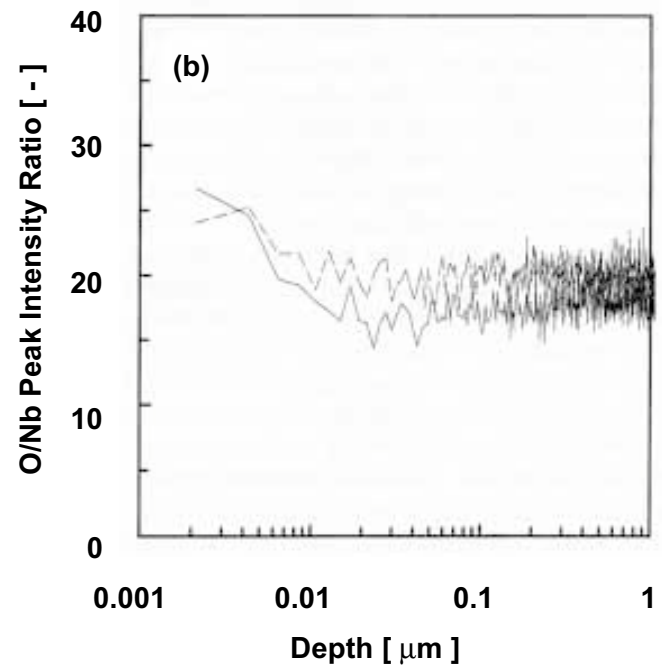
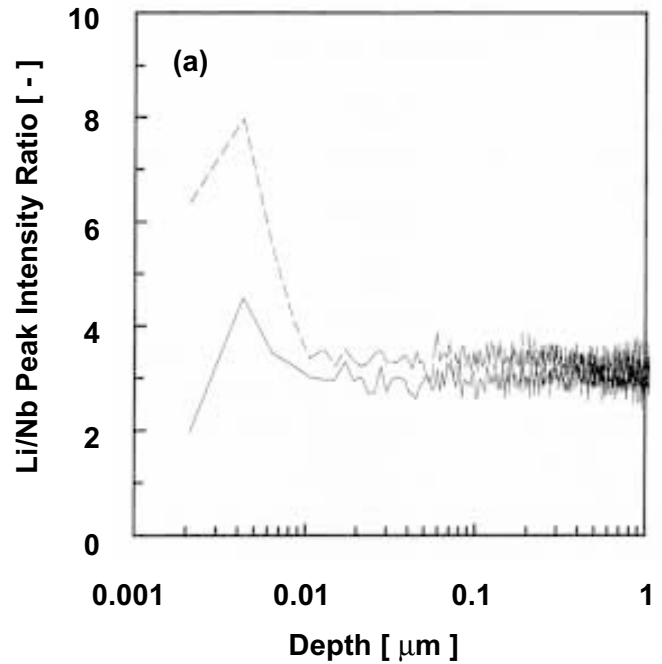


FIG. 3. SIMS peak intensity ratios for (a) Li/Nb and (b) O/Nb. The solid lines denote the unannealed *YW* sample, while the broken lines denote the *YW* sample dry annealed at 1000°C.

for the *NW* [Fig. 5(b)] and *YW* [Fig. 5(c)] samples. No such broadening of the rocking curve was detected for the OH-free sample *ND*, as well as the result after the 1000°C annealing. A possible reason for the partial change of the lattice length, especially for such ionic crystals, is that there was a Coulombic interaction between the contribution ions, some of which were doped into the equilibrium state.

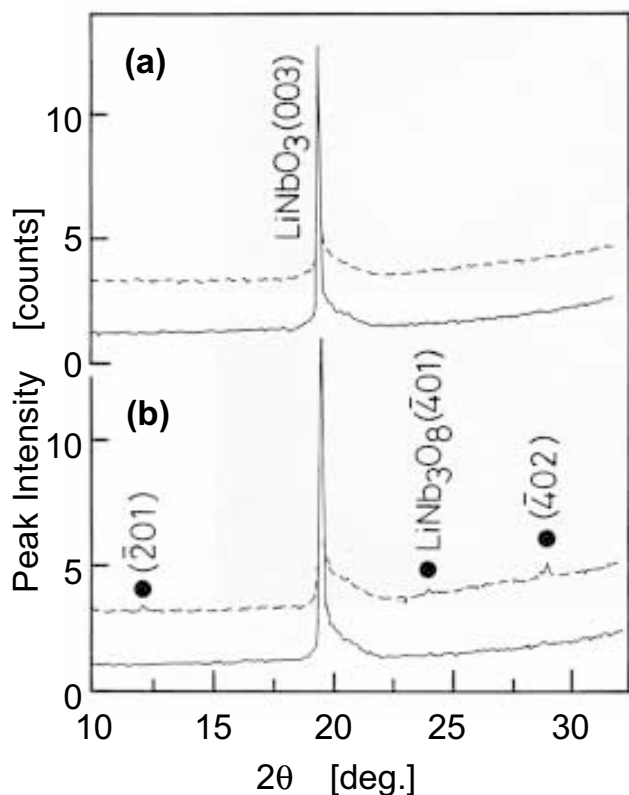


FIG. 4. XRD patterns for the samples (a) *ND* and (b) *YW*. The solid pattern and broken pattern denote the results before and after the dry annealing at 1000°C, respectively. Only in the annealed *YW* samples, broken (b) pattern, weak peaks due to LiNb₃O₈ phase appear.

For instance, the observed lattice contraction due to the dry annealing seemed to be explained by an additional infusion of Li ions into the LiNbO₃.²⁵ In this regard, however, the effects of OH ions (or protons) need to be further investigated. A repulsion between H⁺ and other cations might appear, for instance, leading the lattice extension.

In a LiNbO₃-LiNb₃O₈ system, a reversible phase transformation was known to occur due to the some-what broad solubility of Li₂O into the LiNbO₃.²⁵ The above experimental results indicated that in the OH-free LiNbO₃ substrates, the occurrence of a distortion of the crystallites and an ultimate phase decomposition was successfully suppressed, even after the dry atmosphere annealing. These results supported the expectation by Koide *et al.* that there was correlation between the OH contents in the LiNbO₃ substrate and the moisture contents of the annealing atmosphere necessary to eliminate the LiNb₃O₈ phase.²²

C. AFM observation of dry annealed samples

The AFM observation was carried out for all the samples. Figures 6, 7, and 8 reveal the typical surface morphology of the *ND*, *NW*, and *YW* substrates, respectively. Micrograph (a)

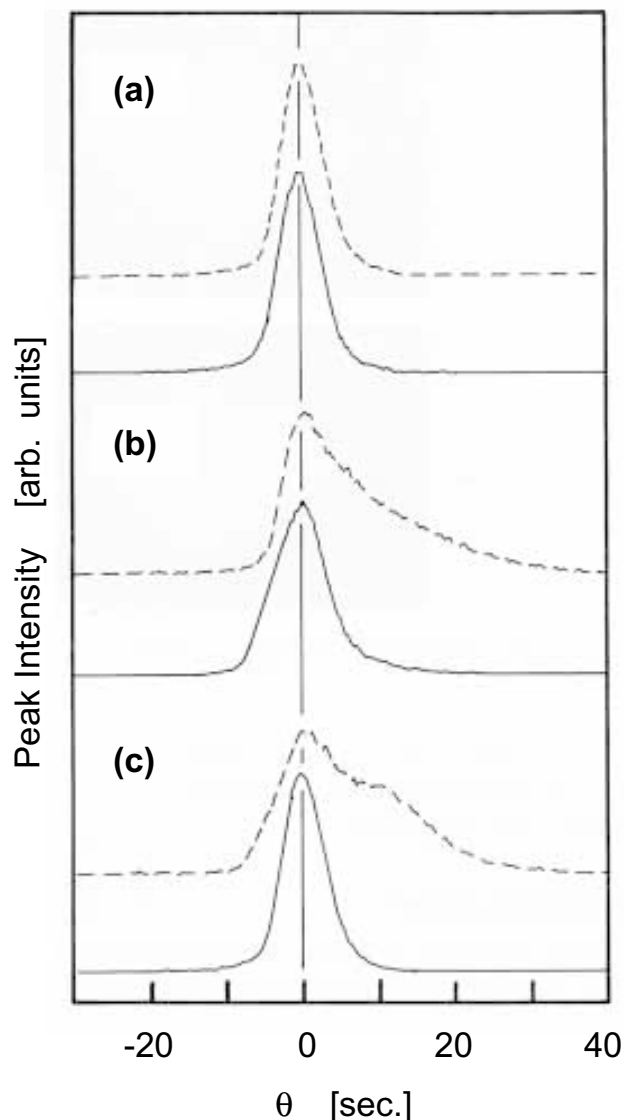


FIG. 5. XRD rocking curves of the (00,12) peak for the samples (a) *ND*, (b) *NW*, and (c) *YW*. The solid curves and broken curves correspond to the results before and after the dry annealing at 800°C, respectively. One division of the horizontal axis denotes 10 s θ angle.

denotes the surfaces before the dry annealing, while micrographs (b), (c), and (d) represent the ones dry annealed at 600, 800, and 1000°C, respectively. It was evident that almost no deterioration in surface morphology was generated for the OH-free *ND* sample even after the 1000 °C annealing. This result was due to an absence of the crystallite distortion and LiNb₃O₈ phase growth in this sample, as described above. In contrast, the step-like coarsening of the annealed *YW* surface seemed to be induced by a regrowth of lithium metaniobate phases due to the chemical and crystalline instability. The observed recovery of FWHM of the XRD rocking

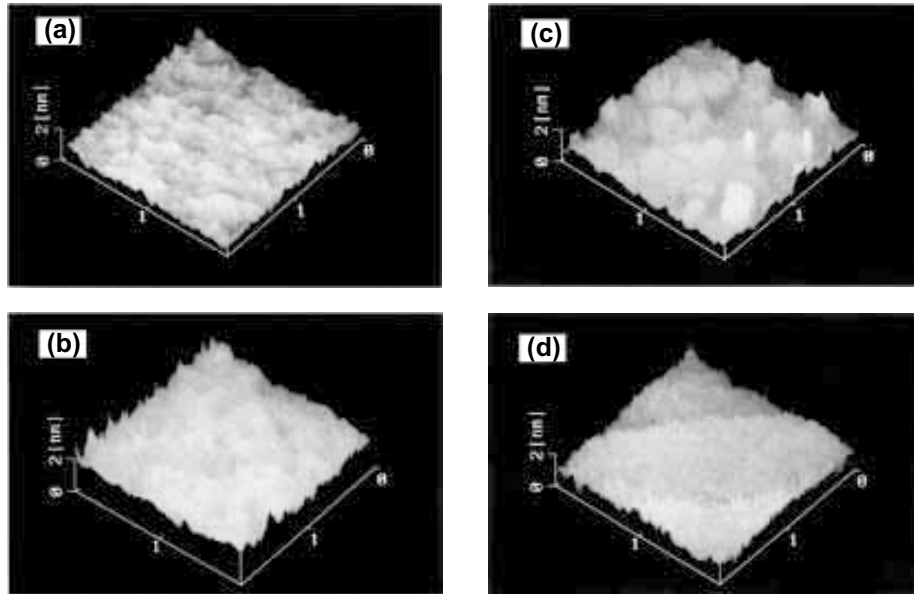


FIG. 6. AFM micrographs of the sample *ND* before the dry annealing (a), and after the dry annealing at 600°C (b), 800°C (c), and 1000°C (d). A scan area is $2 \times 2 \mu\text{m}^2$.

curve from a broad one at 800°C to a sharp one at 1000 °C supported this expectation for the *YW* samples. It is noted that the regain of OH ions also affected the surface morphology of LiNbO₃ [see Fig. 7(a)], although the change of FWHM of XRD rocking curve was small.

IV. CONCLUSIONS

The possibility of the dry atmosphere annealing at 1000 °C without any serious deterioration was experimentally confirmed for the OH-free LiNbO₃ substrates. In the OH-free substrates, unchanged LiNbO₃ crystallite size, the absence of LiNb₃O₈ phase, and surface flatness were observed even after the dry annealing, while the conventional substrate containing greater OH ions was significantly deteriorated in these aspects. The results support that the thermal diffusion pro-

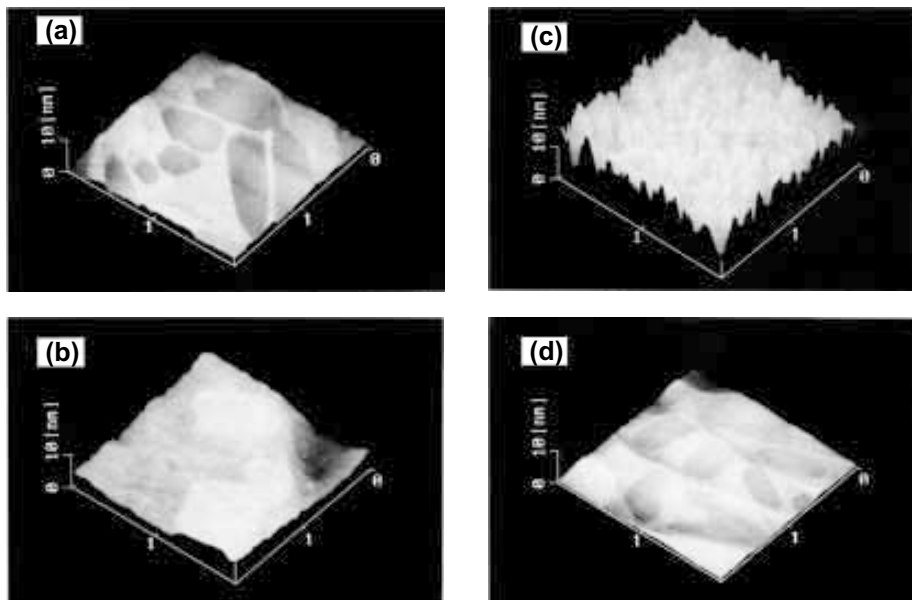


FIG. 7. AFM micrographs of the sample *NW* before the dry annealing (a), and after the dry annealing at 600°C (b), 800°C (c), and 1000°C (d). A scan area is $2 \times 2 \mu\text{m}^2$.

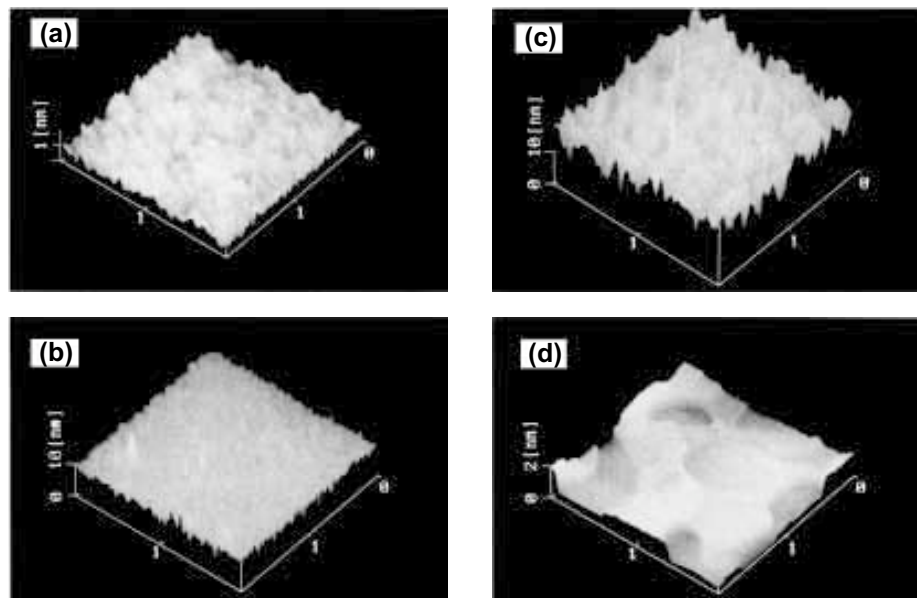


FIG. 8. AFM micrographs of the sample YW before the dry annealing (a), and after the dry annealing at 600°C (b), 800°C (c), and 1000°C (d). A scan area is $2 \times 2 \mu\text{m}^2$.

cess of Ti to prepare optical waveguides under the conventional wet atmosphere could be replaced by a process using dry gases.

ACKNOWLEDGMENTS

The authors would like to thank Mr. Koide of Nihon Kessho Koogaku Co., Ltd. for the helpful information about OH-free LiNbO₃ substrates, Mr. Kinoshita of Chuken Consultant Co., Ltd. for the ICP and ASS measurements of the samples, Dr. Danno and the staff members of UBE Scientific Analysis Laboratory Co. for the thermal analyses of the samples, and Mr. Takano and the staff members of Foundation for Promotion of Material Science and Technology of Japan for the SIMS analyses.

REFERENCES

1. A. M. Yurek, P. G. Suchoski, S. W. Merritt, and F. J. Leonberger, *Optics & Photonics News*, June, 26 (1995).
2. P. G. Suchoski, Jr. and G. R. Boivin, *SPIE* **1795** (Fiber Optic and Laser Sensor X), 38 (1992).
3. L. McCaughan, *SPIE Critical Reviews of Optical Science and Technology* **CR45** (Integrated Optics and Optoelectronics), 15 (1993).
4. E.Y.B. Pun, *ibid.*, 44 (1993).
5. H. Nagata and J. Ichikawa, *Opt. Eng.* **34**, 3284 (1995).
6. D. V. Novikov, T. Gog, M. Griebenow, G. Materlik, I. Baumann, and W. Sohler, *Nucl. Instrum. Methods, Phys. Res. B* **95**, 342 (1995).
7. C. Huang, L. McCaughan, and D. M. Gill, *J. Lightwave Technol.* **12**, 803 (1994).
8. D.M. Gill, J. C. Wright, and L. McCaughan, *Appl. Phys. Lett.* **64**, 2483 (1994).
9. H. Suche, R. Wessel, S. Westenhofer, W. Sohler, S. Bosso, C. Carmannini, and R. Corsini, *Opt. Lett.* **20**, 596 (1994).
10. J.O. Tocho, F. Jaque, J.G. Sole, E. Camarillo, F. Cusso, and J. E. M. Santiuste, *Appl. Phys. Lett.* **60**, 3206 (1992).
11. D. M. Gill, A. Judy, L. McCaughan, and J. C. Wright, *Appl. Phys. Lett.* **60**, 1067 (1992).
12. R. Brinkmann, W. Sohler, and H. Suche, *Electron. Lett.* **27**, 415 (1991).
13. S. Helmfrid, G. Arvidsson, and J. Webjorn, *Electron. Lett.* **27**, 913 (1991).
14. S. Miyazawa and J. Noda, *Oyobutsuri* **48**, 867 (1979) [in Japanese].
15. J. L. Jackel, V. Ramaswamy, and S. P. Lyman, *Appl. Phys. Lett.* **38**, 509 (1981).
16. M. De Sario, M. N. Armenise, C. Canali, A. Camera, P. Mazzoldi, and G. Celotti, *J. Appl. Phys.* **57**, 1482 (1985).
17. M.A. McCoy, S.A. Dregia, and W. E. Lee, *J. Mater. Res.* **9**, 2029 (1994).
18. M. A. McCoy, S.A. Dregia, and W. E. Lee, *J. Mater. Res.* **9**, 2040 (1994).
19. H. Nagata, H. Takahashi, H. Takai, and T. Kougo, *Jpn. J. Appl. Phys.* **34**, 606 (1995).
20. M. Minakata, T. Yonai, and K. Yamada, *CLEO '95*, Baltimore, Maryland, May 21-26, 1995 (Opt. Soc. Am., Washington, DC), Paper CTuD I.
21. R. G. Smith, D. B. Fraser, R.T. Denton, and T. C. Rich, *J. Appl. Phys.* **39**, 4600 (1968).
22. A. Koide, H. Shimizu, and T. Saito, *Jpn. J. Appl. Phys.* **33**, L957 (I 994).
23. H. Nagata, J. Ichikawa, M. Kobayashi, J. Hidaka, H. Honda, K. Kiuchi, and T. Sugamata, *Appl. Phys. Lett.* **64**, I 180 (1994).
24. H. Nagata, J. Ichikawa, N. Mitsugi, T. Sakamoto, T. Shinriki, H. Honda, and M. Kobayashi, *Supplement to Optics & Photonics News* **7** (May, 1996) (Opt. Soc. Am.).
25. A. M. Prokhorov and Yu. S. Kuz'minov, *Physics and Chemistry of Crystalline Lithium Niobate* (Adam Hilger, Bristol, UK, 1990).
26. L. Kovacs, M. Wohlecke, A. Jovanovic, K. Polgar, and S. Kapphan, *J. Phys. Chem. Solids* **52**, 797 (1991).
27. W. Bollmann and H-J. Stohr, *Phys. Status Solidi (a)* **39**, 477 (1977).